**A single-chain antibody generation system yielding CAR-T cells with superior antitumor function**

Toshiki Ochi[1,2], Masaki Maruta[1], Kazushi Tanimoto[1], Fumitake Kondo[1], Toshihiro Yamamoto[3], Mie Kurata[3,4], Hiroshi Fujiwara[1,5], Junya Masumoto[3,4], Katsuto Takenaka[1], Masaki Yasukawa[2,6]

[1]Department of Hematology, Clinical Immunology, and Infectious Diseases, Ehime University Graduate School of Medicine, Toon, Ehime 791-0295, Japan; [2]Division of Immune Regulation, Proteo-Science Center, Ehime University, Toon, Ehime 791-0295, Japan; [3]Department of Analytical Pathology, Ehime University Graduate School of Medicine, Ehime University, Toon, Ehime 791-0295, Japan; [4]Division of Pathology, Proteo-Science Center, Ehime University, Toon, Ehime 791-0295, Japan; [5]Department of Personalized Cancer Immunotherapy, Mie University Graduate School of Medicine, Tsu, Mie 514-8507, Japan; [6]Ehime Prefectural University of Health Sciences, Tobe, Ehime 791-2101, Japan.

**Corresponding author**

Toshiki Ochi, MD, PhD

Department of Hematology, Clinical Immunology and Infectious Diseases,

Ehime University Graduate School of Medicine

Shitsukawa, Toon, Ehime 791-0295, Japan

Phone: +81-89-960-5296

Fax: +81-89-960-5299

E-mail: ochi.toshiki.eg@ehime-u.ac.jp

Supplementary Figure 1

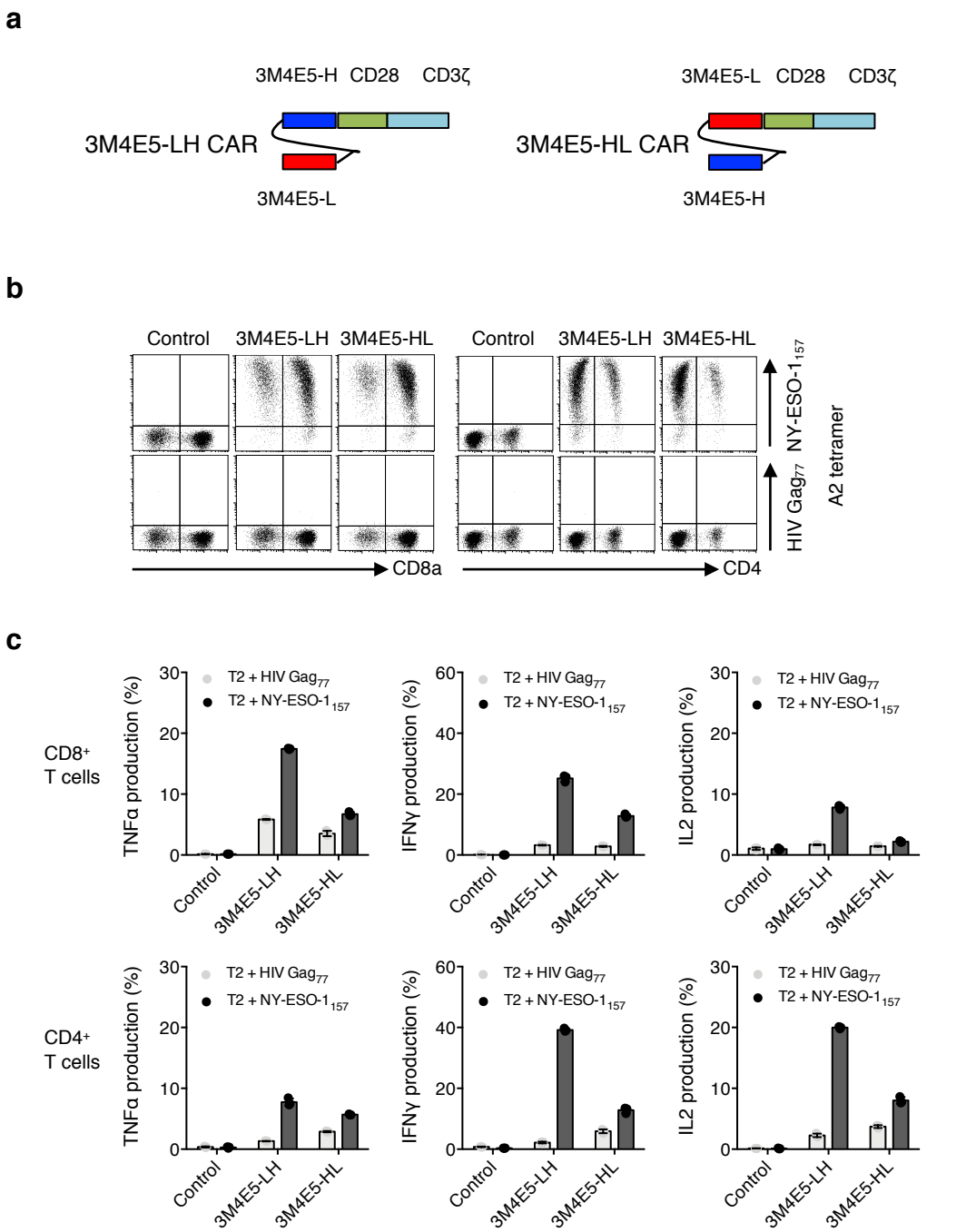

**Supplementary Figure 1. 3M4E5 CAR-T cells recognized A2/NY-ESO-$1_{157}$.**

**a** Second-generation CAR (clone 3M4E5) specific for A2/NY-ESO-$1_{157}$. An A2/NY-ESO-$1_{157}$-specific scFv (3M4E5-LH or 3M4E5-HL) was fused with the CD28 and CD3ζ chains. **b** A2/NY-ESO-$1_{157}$-specific CAR $CD8^+$ T cells and $CD4^+$ T cells were stained with 5 μg/mL A2/NY-ESO-$1_{157}$ tetramer or A2/HIV $Gag_{77}$ tetramer. **c** A2/NY-ESO-$1_{157}$ CAR-T cells were incubated with T2 cells loaded with 10 μg/mL NY-ESO-$1_{157}$ peptide or HIV $Gag_{77}$ peptide, and their cytokine production was measured by intracellular cytokine assays. The experiments were performed in triplicate, and error bars demonstrate the SD.

# Supplementary Figure 2

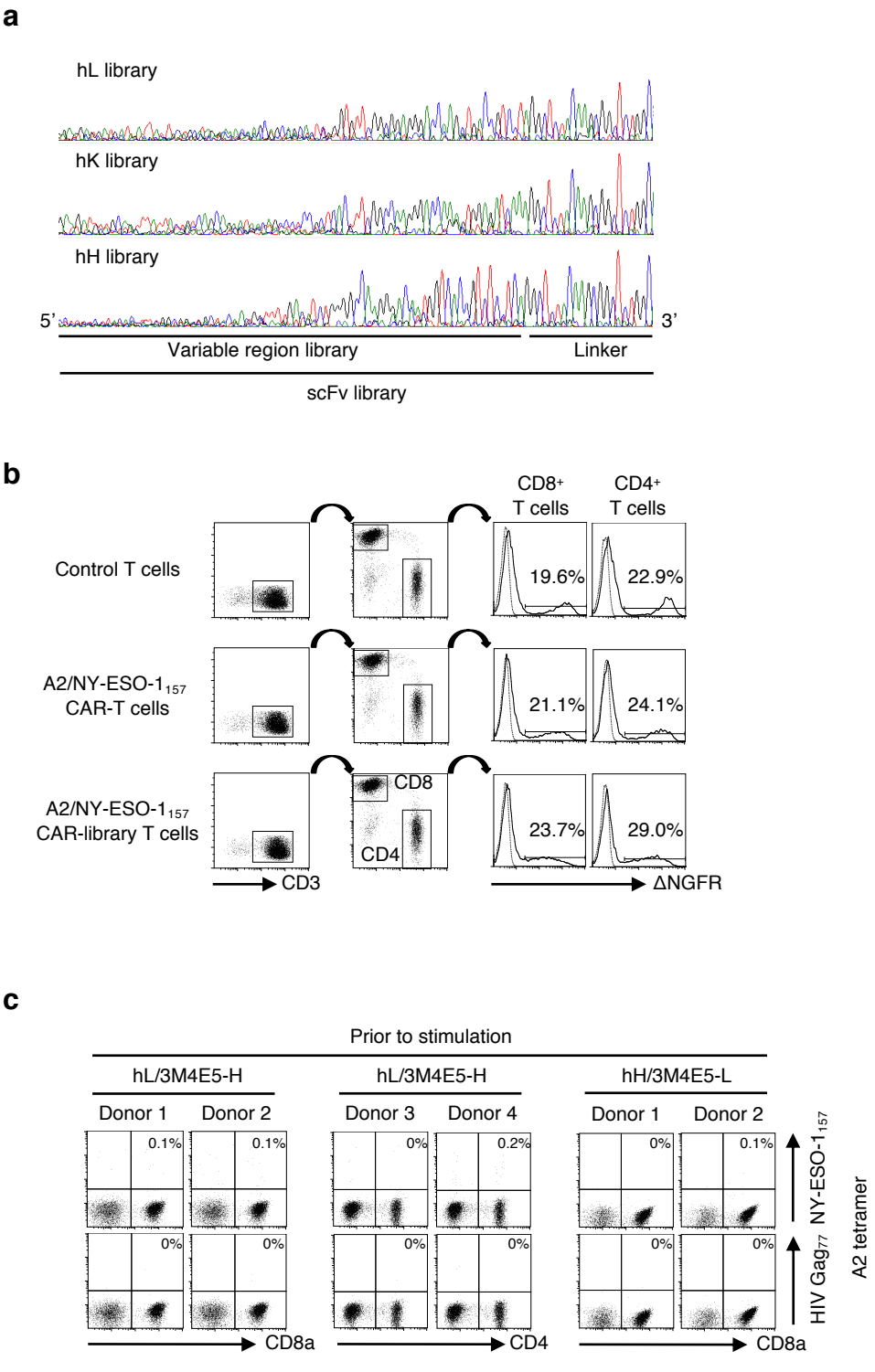

**Supplementary Figure 2. Generation of A2/NY-ESO-$1_{157}$ CAR-library T cells.**

**a** An scFv library in which a variable region library from the lambda chain (hL), kappa chain (hK), or heavy chain (hH) was fused with 3M4E5-H or 3M4E5-L via a linker sequence. A representative chromatogram of each scFv library is shown. **b** Second-generation CAR encoding an scFv library followed by CD28ζ was transduced into peripheral blood T cells. Control T cells and the original A2/NY-ESO-$1_{157}$ CAR-T cells (3M4E5-LH CAR-T cells) were prepared as a negative control and a positive control, respectively. ΔNGFR positivity in gene-modified $CD8^+$ T cells and $CD4^+$ T cells was measured by flow cytometry. The dotted line shows an isotype control. Representative dot plots and histograms are depicted. **c** A2/NY-ESO-$1_{157}$ CAR-library T cells prior to stimulation were stained with 20 μg/mL A2/NY-ESO-$1_{157}$ tetramer or A2/HIV $Gag_{77}$ tetramer, and each dot plot is shown. Each percentage of A2/NY-ESO-$1_{157}$ tetramer-positive cells among CAR-library T cells is shown. Stainings of the A2/NY-ESO-$1_{157}$ CAR-library T cells after antigen-specific stimulation are depicted in Fig. 2a.

Supplementary Figure 3

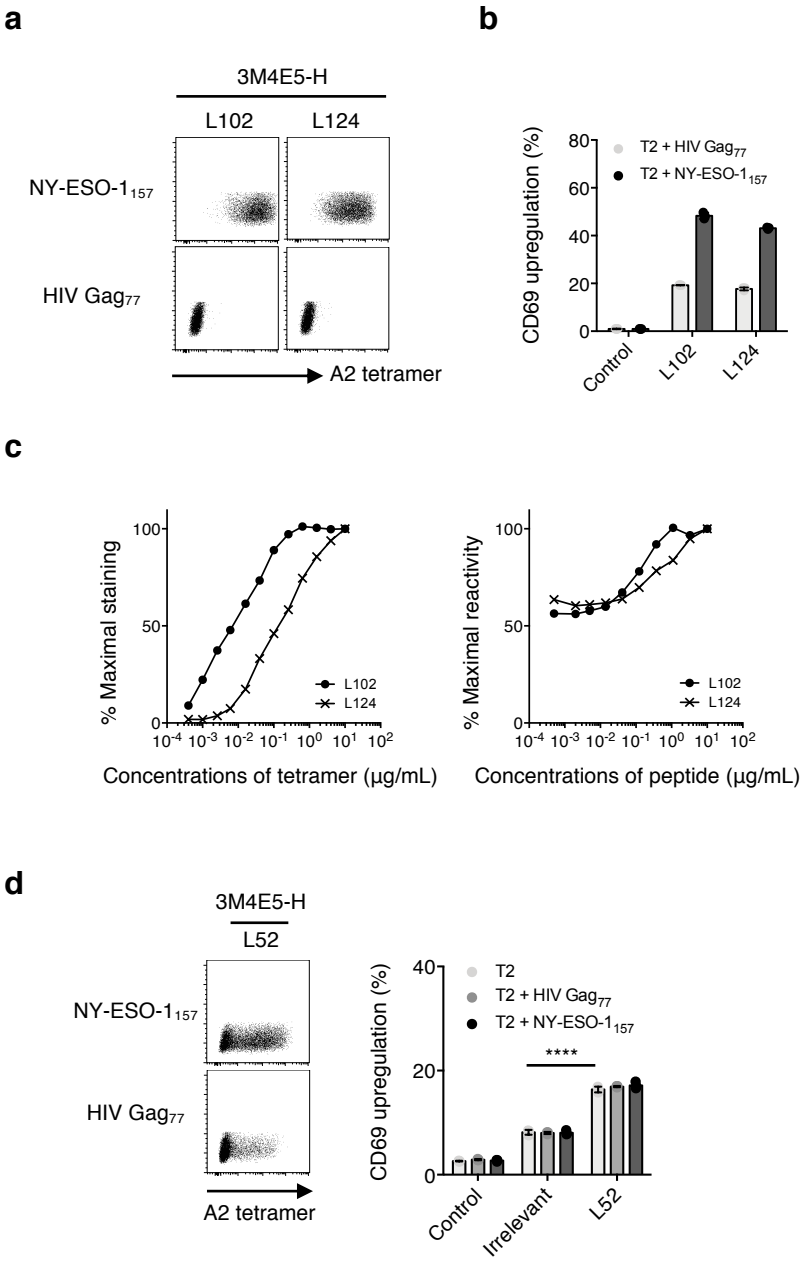

**Supplementary Figure 3. Characteristics of new scFv-expressing A2/NY-ESO-$1_{157}$ CAR-T cells.** **a** CAR encoding a new light chain (L102, or L124) paired with 3M4E5-H was individually reconstituted in Jurkat 76 cells. Jurkat 76/CAR transfectants were stained with 5 μg/mL A2/NY-ESO-$1_{157}$ tetramer or A2/HIV $Gag_{77}$ tetramer. **b** Jurkat 76/CAR transfectants were incubated with T2 cells pulsed with 10 μg/mL NY-ESO-$1_{157}$ peptide or HIV $Gag_{77}$ peptide. CD69 upregulation of the transfectants was measured by flow cytometry. The experiments were performed in triplicate, and error bars show the SD. **c** Jurkat 76/CAR transfectants were stained with graded concentrations of A2/NY-ESO-$1_{157}$ tetramer (left). They were also incubated with T2 cells pulsed with graded concentrations of A2/NY-ESO-$1_{157}$ peptide (right). Percentage maximal staining and percentage maximal reactivity of each transfectant was calculated, similarly to Fig. 2f. **d** The Jurkat 76/CAR transfectant expressing clone L52 paired with 3M4E5-H as the scFv was stained with 5 μg/mL A2/NY-ESO-$1_{157}$ or A2/HIV $Gag_{77}$ tetramer. CD69 upregulation of L52 CAR-T cells, irrelevant CAR-T cells, and control T cells was also measured by flow cytometry. The experiments were performed in triplicate, and error bars show the SD. Welch's t test (two-sided) was performed for comparison. ****, $p < 0.0001$.

Supplementary Figure 4

**a**

| Peptide | Sequence | Binding affinity (nM) |
|---|---|---|
| NY-ESO-$1_{157\text{-}165}$ | SLLMWITQC | 666.69 |
| LYPLAL$1_{36\text{-}44}$ | GLRMWIKQV | 1859.63 |

**b**

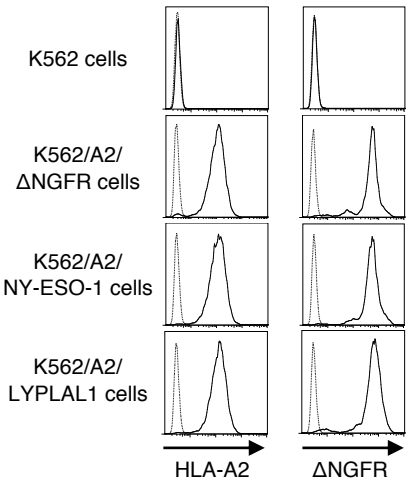


**c**

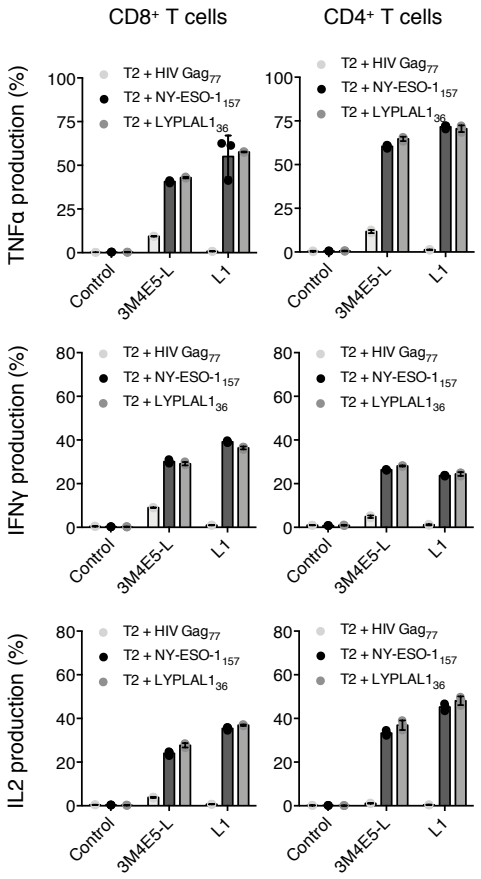


**d**

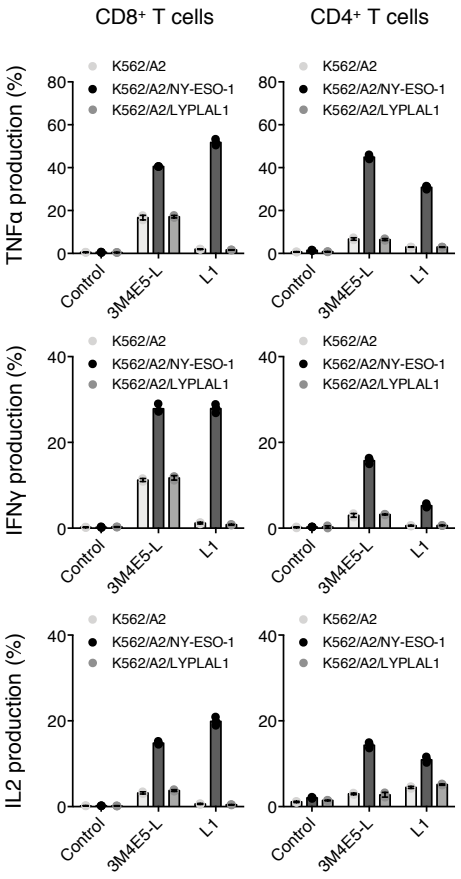

**Supplementary Figure 4. Assessment of potential cross-reactivity mediated by L1 CAR-T cells.** **a** Based on the peptide sequence motif (xLxMWIxQx) revealed by alanine scanning assays, one potential cross-reactive peptide, LYPLAL1$_{36\text{-}44}$, was identified. The amino acid sequences of NY-ESO-1$_{157}$ and LYPLAL1$_{36}$ peptides, and their predicted binding capacity to HLA-A*02:01 using netMHC4.0 (http://www.cbs.dtu.dk/services/NetMHC/) are also shown. **b** HLA-A2 and ΔNGFR expressions of K562 cells, K562/A2 cells, K562/A2/NY-ESO-1 cells, and K562/A2/LYPLAL1 cells were assessed by flow cytometry. The *ΔNGFR* gene was employed as a tag gene, as described in Methods. The dotted line shows an isotype control. **c, d** L1 CAR-T cells and 3M4E5-L CAR-T cells were incubated with T2 cells loaded with 10 μg/mL NY-ESO-1$_{157}$ peptide, LYPLAL1$_{36}$ peptide, or HIV Gag$_{77}$ peptide (**c**). Then, these CAR-T cells were cocultured with K562-based target cells (**d**). Cytokine production by CAR-T cells was assessed using intracellular cytokine assays. The experiments were performed in triplicate, and error bars demonstrate the SD. The control T cells and CAR-T cells were prepared and analyzed similarly to Fig. 3.

Supplementary Figure 5

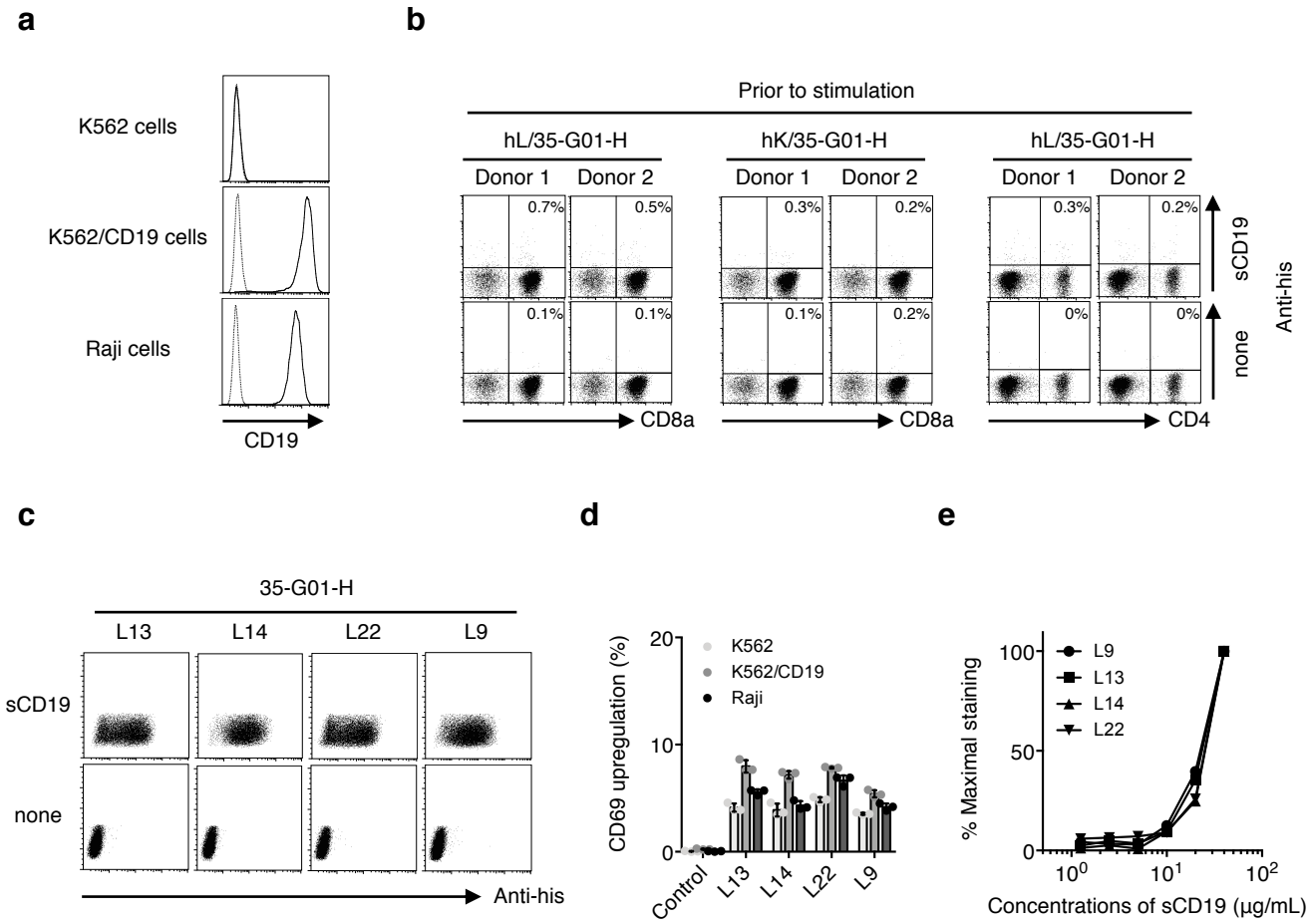

**Supplementary Figure 5. Characteristics of new scFv-expressing CD19 CAR-T cells.**

**a** CD19 expression of K562 cells, K562/CD19 cells, and Raji cells was assessed by flow cytometry. The dotted line shows an isotype control. **b** CD19 CAR-library T cells prior to stimulation were stained with 40 μg/mL sCD19 dimer or PE-anti-his mAb alone, and each dot plot is shown. Each percentage of sCD19 dimer-positive cells among CAR-library T cells is displayed. Stainings of the CD19 CAR-library T cells after antigen-specific stimulation are depicted in Fig. 4c. **c** CAR encoding newly isolated light chains (L13, L14, L22, or L9) paired with 35-G01-H was individually reconstituted in Jurkat 76 cells. Jurkat 76/CAR transfectants were stained with 40 μg/mL sCD19 dimer or PE-anti-his mAb alone. **d** Jurkat 76/CAR transfectants were incubated with the indicated target cells, and their CD69 upregulation was examined by flow cytometry. The experiments were performed in triplicate, and error bars show the SD. **e** Jurkat 76/CAR transfectants were stained with graded concentrations of sCD19 dimer. Percentage maximal staining was calculated, similarly to Fig. 4g.

Supplementary Figure 6

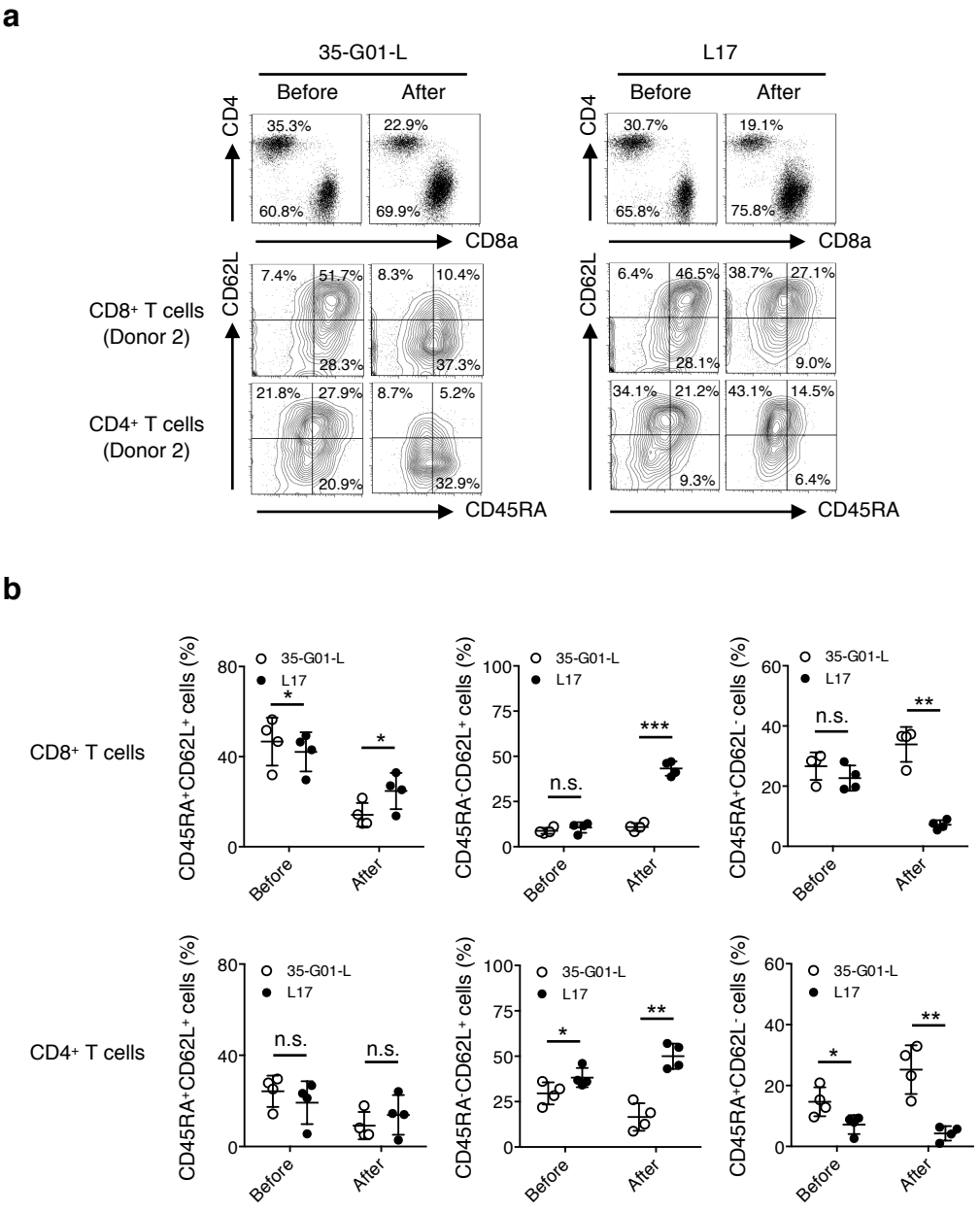

**Supplementary Figure 6. T-cell phenotypes of CD19 CAR-T cells after stimulation.**

**a** The positivity of $CD8^+$ and $CD4^+$ T cells among L17, or 35-G01-L CAR-T cells derived from donor 2 before and after stimulation with Raji cells is shown (top). The proportions of CD45RA and/or CD62L-positive cells among L17, or 35-G01-L CAR $CD8^+$ T cells and $CD4^+$ T cells (donor 2) are also depicted, respectively (middle, bottom). **b** The percentages of $CD45RA^+CD62L^+$, $CD45RA^-CD62L^+$, and $CD45RA^+CD62L^-$ cells among CAR $CD8^+$ T cells and $CD4^+$ T cells of 4 different donors before and after stimulation are shown. Each dot depicts the percentage of the indicated population among CAR-T cells generated from each donor. Differences between L17 and 35-G01-L CAR-T cells were statistically analyzed by paired t test (two-sided). *, $p < 0.05$; **, $p < 0.01$; ***, $p < 0.001$; n.s., not significant.

Supplementary Figure 7

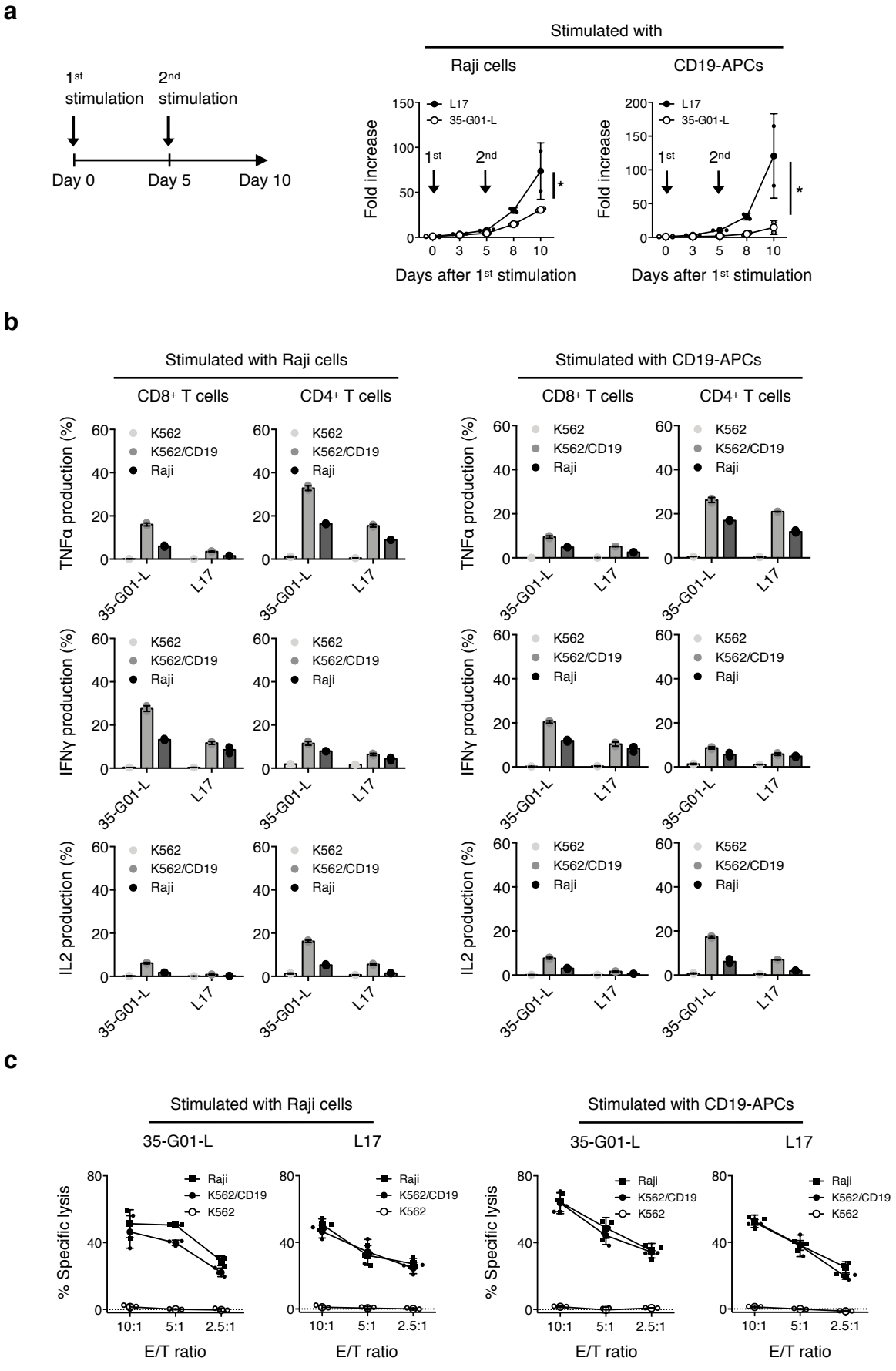

**Supplementary Figure 7. Characteristics of CD19 CAR-T cells repeatedly stimulated with $CD19^+$ target cells.**

**a** L17 and 35-G01-L CAR-T cells were stimulated twice with Raji cells (E/T 1:1) or CD19-APCs (E/T 10:1) on Day 0 and Day 5 (left). The fold increase of CAR-T cells established from 2 different donors after the first stimulation is shown (right). Arrows inside the graphs indicate the time point of stimulation. Error bars indicate the SD. Two-way ANOVA with Sidak's correction was conducted for multiple comparisons. *, $p < 0.05$. **b** Cytokine production by L17, and 35-G01-L CAR-T cells against the indicated target cells following two stimulations was assessed using intracellular cytokine assays. The experiments were performed in triplicate, and error bars show the SD. **c** Cytotoxicity of expanded L17 and 35-G01-L CAR-T cells against target cells was examined by $^{51}Cr$-release assays. The experiments were performed in triplicate, and error bars depict the SD.

# Supplementary Figure 8

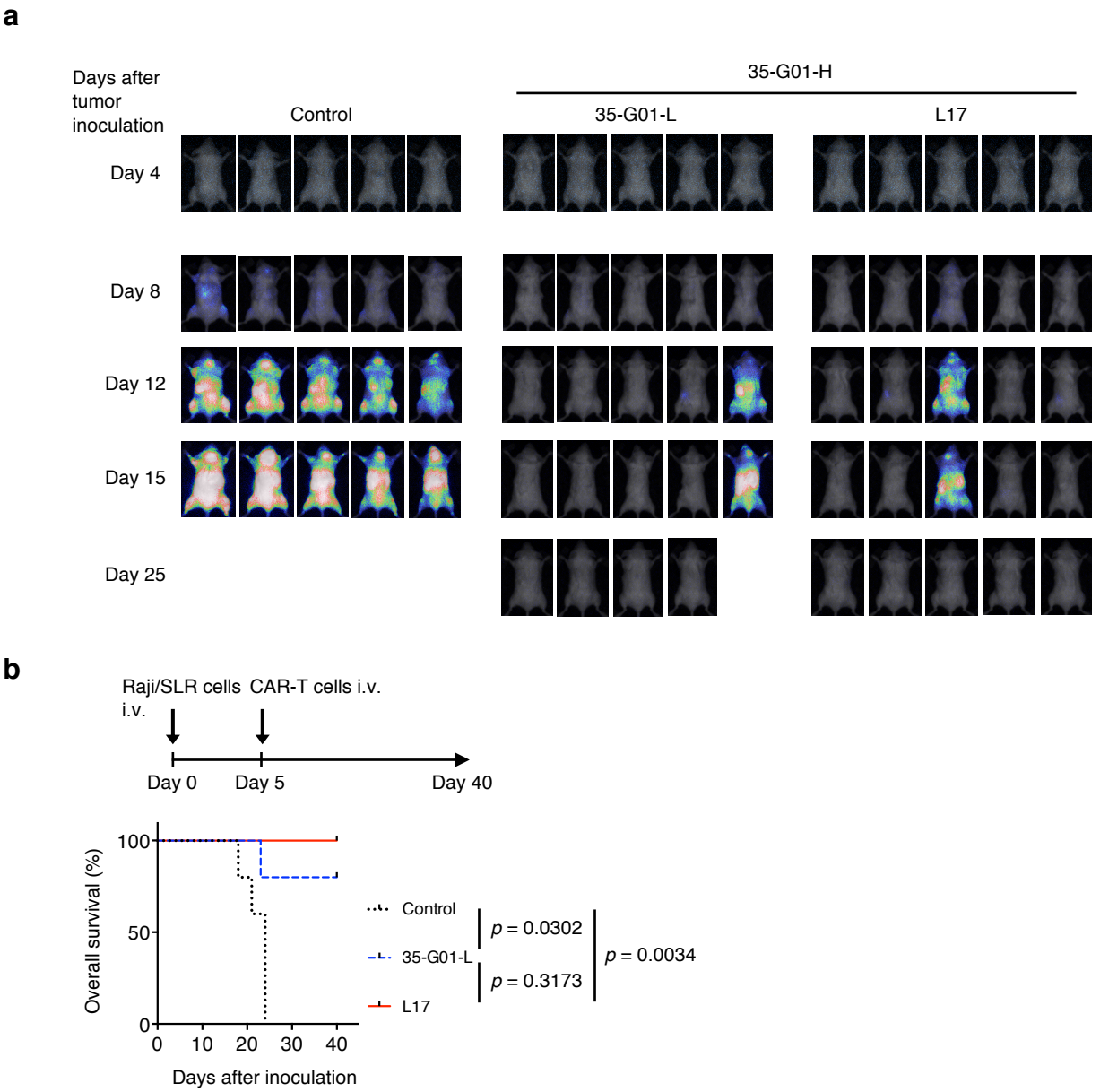

**Supplementary Figure 8. *In vivo* antitumor effects of CD19 CAR-T cells.**

**a, b** Five hundred thousand Raji/SLR cells were intravenously injected into irradiated NOD/Shi-scid IL2rgamma(null) mice. After confirming the engraftment of Raji/SLR cells by bioluminescence imaging assays on Day 4, $2.0 \times 10^6$ CAR-T cells or control T cells were intravenously injected on Day 5. Photon images of mice on Days 8, 12, 15, and 25 are shown (**a**). The treatment schedule is summarized, and the overall survival of each group (n = 5 mice per group) is represented and compared in the form of a Kaplan-Meier curve, similarly to Fig. 6a. Log-rank (Mantel-Cox) test was performed, and *p* values are also shown (**b**).

Supplementary Figure 9

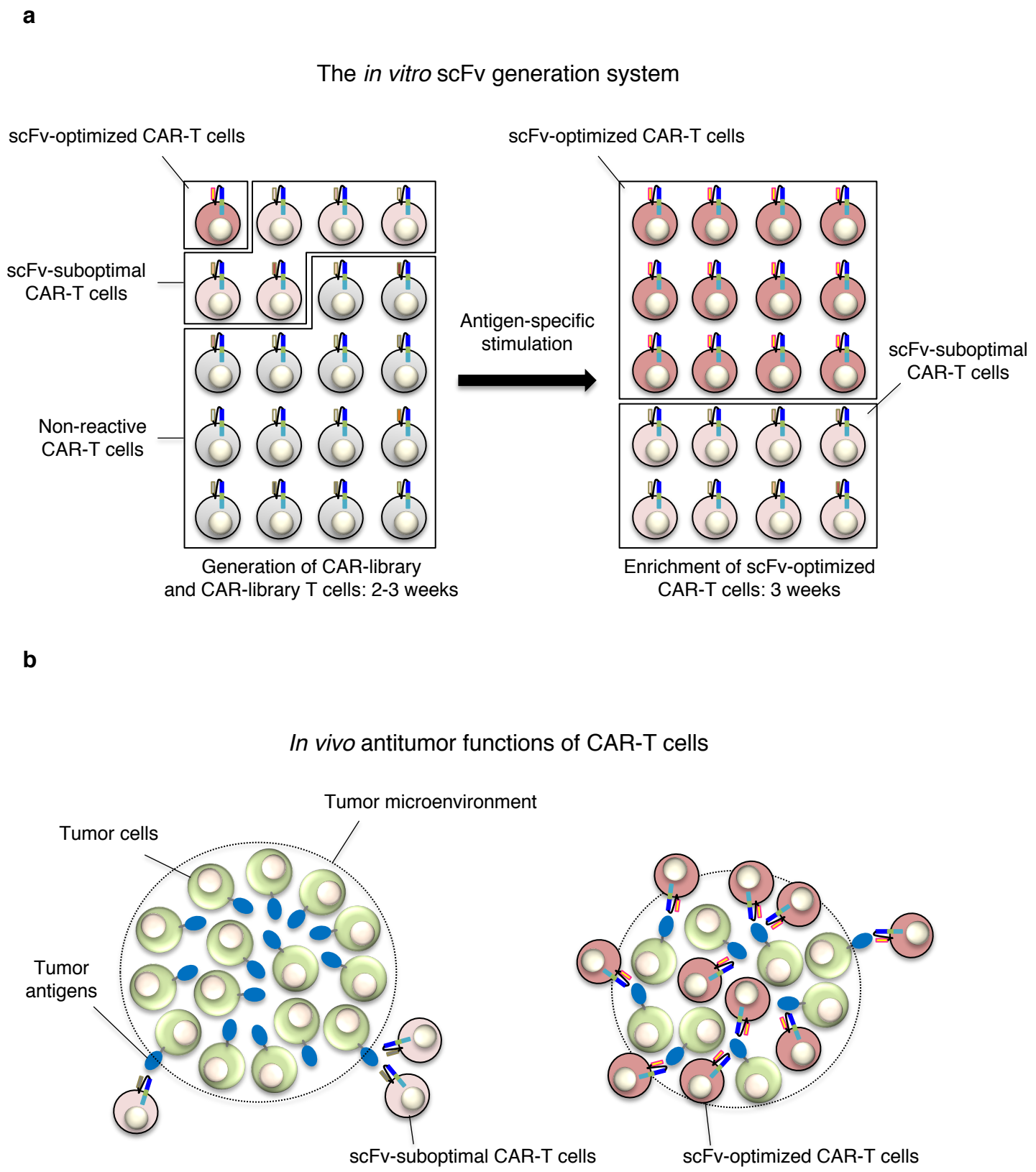

**Supplementary Figure 9. The *in vitro* scFv generation system potentially yielding CAR-T cells with superior *in vivo* antitumor function.**

**a** The *in vitro* scFv generation system using CAR-library T cells. ScFv-optimized (dark red), scFv-suboptimal (light red), and non-reactive (gray) CAR-T cells are included among CAR-library T cells (left). Since scFv-optimized CAR-T cells have a survival and proliferation advantage over scFv-suboptimal CAR-T cells after antigen-specific stimulation of CAR-library T cells, the former appears to be well concentrated, allowing identification of new scFvs that can endow CAR-T cells with superior antitumor function *in vivo* (right). The times required for generation of CAR-library and CAR-library T cells and enrichment of scFv-optimized CAR-T cells are shown similarly to Fig. 1. The supporting data are shown in Fig. 5, Supplementary Fig. 6, 7. **b** The cartoons summarize the results shown in Fig. 6. ScFv-suboptimal CAR-T cells (light red) appear to be localized around the tumor site *in vivo* (left), whereas scFv-optimized CAR-T cells (dark red) seem to infiltrate diffusely and accumulate within the tumor, recognizing and killing tumor cells *in vivo* (right). These *in vivo* antitumor effects may be explained by sufficient antitumor cytotoxicity, superior proliferation capacity, and durable phenotypes of CAR-T cells expressing the scFv optimized by our *in vitro* scFv generation system.

Supplementary Table 1

| Clone | Variable region | CDR3 | J region | Structural avidity ($EC_{50}$: μg/mL) | Functional avidity ($EC_{50}$: μg/mL) |
|---|---|---|---|---|---|
| **Variable regions of light chain (lambda chain) pairing with 3M4E5-H** | | | | | |
| 3M4E5-L | 2-11*01 | CWSFAGSYYVF | 1*01 | 0.002 | 0.162 |
| L1 | 2-8*01 | CSSYAGSNSVF | 1*01 | 0.005 | 0.031 |
| L102 | 2-8*01 | CSSYAGSGSTPFVF | 1*01 | 0.017 | 0.122 |
| L73 | 2-14*01 | CSSYSGSSTWVF | 3*02 | 0.036 | 0.270 |
| L124 | 2-14*01 | CCSYAGRRYVF | 1*01 | 0.141 | 0.624 |
| L88 | 2-11*01 | CCSYAGGYYVF | 1*01 | 0.171 | 0.459 |
| L66 | 2-14*01 | CSSYTSSSTYVF | 1*01 | 1.197 | 0.997 |
| L80 | 2-14*02 | CSSYTSSSTFAVF | 7*01 | NC | NC |
| L52 | 1-40*01 | CGTWDSSLSAGVF | 7*01 | NC | NC |
| **Variable regions of heavy chain pairing with 3M4E5-L** | | | | | |
| 3M4E5-H | 3-23*01 | CAGELLPYYGMDVW | 6*02 | 0.009 | 0.248 |
| H73 | 4-34*09 | CARCPIYYYGMDVW | 6*02 | 0.016 | 0.043 |
| H1 | 4-59*01 | CARESYYYYGMDVW | 6*02 | 0.066 | 0.065 |

**Supplementary Table 1. Variable regions and CDR3 sequences of A2/NY-ESO-$1_{157}$-specific VL and VH, and characteristics of CAR-T cells expressing each scFv.**

According to the nomenclature of the IMGT (http://www.imgt.org/), the variable regions and amino acid sequences of the CDR3 region of newly identified and original light chains and heavy chains specific for A2/NY-ESO-$1_{157}$ are summarized. The structural avidity and functional avidity of Jurkat 76/CAR-T cells expressing each scFv are shown as the $EC_{50}$ value (μg/mL), measured as described in Fig. 2. NC, not calculated.

Supplementary Table 2

| Clone | Variable region | CDR3 | J region | Structural avidity ($EC_{50}$: μg/mL) |
|---|---|---|---|---|
| **Variable regions of light chain (lambda chain) pairing with 35-G01-H** | | | | |
| 35-G01-L | 2-8*01 | CCSYAGRYNSVLF | 2*01 | 9.92 |
| L17 | 1-47*01 | CAAWDDSLSAIF | 2*01 | 11.98 |
| L16 | 2-8*01 | CAAWDDSLNGVVF | 2*01 | 16.28 |
| L7 | 2-11*01 | CGTWDTSLTAVVF | 2*01 | 17.93 |
| L9 | 1-51*01 | CGTWESSLSGVVF | 2*01 | 18.84 |
| L13 | 2-14*01 | CSSYTTSTTWVF | 3*02 | 19.23 |
| L14 | 2-14*01 | CCSYAGSYTFVVF | 2*01 | 20.91 |
| L22 | 2-14*01 | CHSYDSSLSHVF | 1*01 | 21.31 |
| L4 | 3-1*01 | CQAWDSSTHVVF | 2*01 | 21.58 |
| **Variable regions of light chain (kappa chain) pairing with 35-G01-H** | | | | |
| K5 | 3-11*01 | CQQSYSTLLYTF | 2*01 | 12.97 |
| K4 | 3-15*01 | CQQYNNWPPLYTF | 2*01 | 13.37 |
| K9 | 3-20*02 | CQQFNEWPLTF | 4*01 | 15.38 |
| K6 | 3-15*01 | CQQYDSLPLTF | 4*01 | 18.01 |

**Supplementary Table 2. Variable regions and CDR3 sequences of CD19-specific VL, and characteristics of CAR-T cells expressing each scFv.**

Based on the nomenclature of the IMGT (http://www.imgt.org/), the variable regions and amino acid sequences of the CDR3 region of newly isolated and original light chains specific for CD19 are listed. The structural avidity of CAR-T cells possessing each scFv is shown as the $EC_{50}$ value (μg/mL), calculated as the concentration of sCD19 dimer required to achieve 50% of the maximal staining.